



Novel Poly Deep Eutectic Solvents Based Supported Liquid Membranes for CO₂ Capture

Manzar Ishaq¹, Mazhar Amjad Gilani², Zobila Muhammad Afzal², Muhammad Roil Bilad³, Abdul-Sattar Nizami⁴, Mohammad Rehan⁵, Eza Tahir⁴ and Asim Laeeq Khan^{1*}

¹Department of Chemical Engineering, COMSATS University Islamabad, Islamabad, Pakistan, ²Department of Chemistry, COMSATS University Islamabad, Islamabad, Pakistan, ³Chemical Engineering Department, Universiti Teknologi PETRONAS, Perak, Malaysia, ⁴Sustainable Development Study Centre, Government College University, Lahore, Pakistan, ⁵Center of Excellence in Environmental Studies (CEES), King Abdulaziz University, Jeddah, Kingdom of Saudi Arabia

The poly deep eutectic solvents (PDESs), a potential substituent to ionic liquids, have emerged as relatively new material and have been successfully applied in catalysis, nanotechnology, and, more importantly, in gas separation. Herein, the PDESs were incorporated for the first time in the CO₂ capturing membranes to exploit their inherent advantages in the acid gas capture. The PDESs were synthesized by mixing choline chloride (hydrogen bond acceptor-HBA) and two hydrogen bond donors-HBDs (polyacrylic acid and polyacrylamide) separately in different molar ratios. The physical changes of the resulting homogeneous mixture along with the Fourier Transform Infrared confirmed the successful synthesis of the PDESs. Afterward, these PDESs were impregnated into microporous polyvinylidene fluoride (PVDF) membrane support to fabricate supported liquid membranes (SLMs). The gas performance of the prepared PDES-SLMs was tested under pure and mixed-gas conditions for CO₂, CH₄, and N₂. The PDES-SLMs showed a significantly high CO₂/CH₄ and CO₂/N₂ selectivities of the order of 55.5 and 60, respectively. To evaluate their practical implication, the SLMs were investigated systematically under different operating conditions such as choline content, temperature, volume fraction of the CO₂ in the feed, and the activation energy required for CO₂ capture. The synthesized SLMs showed exceptional results in both permeability and selectivity viewpoint. The remarkable SLMs gas performance can be ascribed to the basicity, molar free volume, and the H-bonding strength of the synthesized PDESs. The green potential, low cost, and the promising gas separation performance make these PDESs a favorable alternative to the competing PILs in capturing the greenhouse acid gases.

OPEN ACCESS

Edited by:

Hu Li,
Guizhou University, China

Reviewed by:

Hu Pan,
Jiaxing University, China
Anping Wang,
Guizhou Normal University, China

*Correspondence:

Asim Laeeq Khan
alaeqkhan@cuilahore.edu.pk

Specialty section:

This article was submitted to
Bioenergy and Biofuels,
a section of the journal
Frontiers in Energy Research

Received: 14 August 2020

Accepted: 23 September 2020

Published: 30 October 2020

Citation:

Ishaq M, Gilani MA, Afzal ZM, Bilad MR, Nizami A-S, Rehan M, Tahir E and Khan AL (2020) Novel Poly Deep Eutectic Solvents Based Supported Liquid Membranes for CO₂ Capture. *Front. Energy Res.* 8:595041. doi: 10.3389/fenrg.2020.595041

Keywords: carbon dioxide capture, poly deep eutectic solvents, supported liquid membrane, permeability, selectivity

Abbreviations: PDES, poly deep eutectic solvents; DES, deep eutectic solvents; PIL, polymerized ionic liquid; IL, ionic liquid; HBA, hydrogen bond acceptor; HBD, hydrogen bond donor; PAA, polyacrylic acid; PAM, polyacrylamide; ChCl, choline chloride; Ea, activation energy

INTRODUCTION

The carbon dioxide (CO₂), primarily released to the environment by the consumption of fossil fuels and other major industrial processes, contributes to 60% of the greenhouse gases and, posing the threat of global warming (Coninck et al., 2005). As a result, there is an urgent requirement of effective CO₂ capturing technologies to control the emissions of greenhouse gases. Primarily there are three methods of CO₂ capturing, i.e., Pre-combustion, Post-combustion, and oxy-fuel method. The conventional technologies for CO₂ suppression include cryogenic distillation, adsorption, and absorption. In the cryogenic distillation, CO₂ is captured at low temperature, and the process involves compression and expansion of the CO₂, and at the end, liquefied CO₂ is obtained. This technology has limitations of high energy consumption, special equipment requirement, and small concentration of CO₂, which make the process uneconomical as it cannot be used at a large scale. The absorption method usually employs the amine-based porous adsorbents for CO₂ capturing. This process involves both physisorption and chemisorption of the acid gas. The main disadvantage of the adsorption method is difficult regeneration and scarcity of suitable adsorbents (Shen et al., 2020). In the absorption technique, CO₂ is separated based on solubility in the solvent. CO₂ is absorbed in a solvent, then separated from the solvent at high temperature, and solvent is regenerated. The absorption could be physical or chemical. The main issue with absorption technology is high energy requirement and the need for particular green solvents with high CO₂ solubility values (de Almeida Quintino, 2014; Songolzadeh et al., 2014). These techniques are energy intensive because of the solvent regeneration and elevated operating conditions (Tuinier et al., 2010; Wang et al., 2011). The membrane technology provides numerous advantages over other conventional techniques such as eco-friendliness, low energy demand, ease of operation, and one-step separation (Bernardo et al., 2009; Peng et al., 2014; Pan et al., 2020). In particular, the supported liquid membranes (SLMs), especially supported ionic liquid membranes (SILMs) have been investigated broadly, which combine the highly processable and flexible polymeric support impregnated with ionic liquids (ILs) for CO₂ capture (Malik et al., 2011; Uchytel et al., 2011).

The inherent advantages of ILs such as high thermal stability, extremely low vapor pressure, and non-flammability, make them suitable options for CO₂ capture (Meine et al., 2010; Emel'yanenko et al., 2014). Additionally, the relatively new idea of combining polymer and IL as polymerized ionic liquid (PIL) membranes was put forward by Bara et al. for the first time in 2007 (Bara et al., 2007). The PIL membranes share the advantageous properties of ILs along with high mechanical stability of the membranes under high pressure. However, the CO₂ permeabilities of these PIL dense membranes were found to be significantly lower because of low diffusion rate of the acid gas through them (Bara et al., 2007; Bara et al., 2008a). The PIL based SLMs have also been fabricated and investigated for their potential in increasing CO₂ permeability and CO₂/light gas selectivity by relying on the solubility selectivity (Bara et al., 2008b; Bara et al., 2009b; McDanel et al., 2014). Despite these

many advantages discussed above, several drawbacks of ILs have also been articulated, such as extremely high viscosity, toxicity, synthesis cost, and non-biodegradability (Pham et al., 2010; Biczak et al., 2014). Therefore, there is a need for green substituent of ILs in the field of SLM that can selectively separate the acid gas from the mixture of gases.

In this context, deep eutectic solvents (DESs), obtained because of hydrogen bonding formed between the hydrogen bond acceptor (HBA) and hydrogen bond donor (HBD), are a promising alternative (Francisco et al., 2013; García et al., 2015). The melting point of the DESs lies far below the melting points of the individual precursors, which is a characteristic feature of the eutectic solvents. The characteristic properties of the DESs can also be tuned according to the application requirement by altering the choice of HBA and HBD and their molar ratios (García et al., 2015). The DESs have many advantages compared to ILs, such as cost-effectiveness, biodegradability, ease of synthesis, and biocompatibility (Smith et al., 2014). The very first DES reported by Abbott et al. was formed between choline chloride-HBA (a vitamin B component) and urea-HBD (Abbott et al., 2003). Afterward, most of the DESs reported were primarily obtained from the choline chloride because it is a biodegradable and low cost, as the price of choline based DESs is merely 4–9% of the conventional ILs (Ma et al., 2018).

In the past decade, a plethora of review articles on CO₂ absorption by the DESs have been published so far, showing high DESs affinity for CO₂ (García et al., 2015; Aissaoui et al., 2017; Sarmad et al., 2017; Zhang et al., 2018). The polymerized deep eutectic solvents (PDESs), are a new class of DESs in which the HBD part is polymerizable (Zhang et al., 2012; Mota-Morales et al., 2013; Ren'ai et al., 2018). PDESs have also been investigated like PILs, for CO₂ capture in the absorption process by Isik et al. (Isik et al., 2016a; Isik et al., 2016b), showed significantly high CO₂ uptakes. The polymerizable HBD was employed to synthesize PDESs for CO₂ absorption process, while the HBD was polymerized using photo polymerization. The results of the investigations revealed that the PDESs are excellent CO₂ sorbents (Isik et al., 2016a; Isik et al., 2016b). However, the risk of a complete conversion of the HBD to polymerized HBD and the maintenance of HBA-HBD interactions cannot be neglected.

To the best of our knowledge, PDESs have never been investigated in membrane-based CO₂ capturing. The ambition behind this study is the findings of molecular dynamics simulation work investigated by Shen and Hung (2017), which revealed that the DESs family could efficiently be incorporated in the porous support of SLMs for CO₂ capture. Therefore, this study, for the first time, used polymerized HBD to make DES with the HBA to avoid the risk of incomplete polymerization; plus the energy requirements reduced significantly for such chemistry. Polyacrylic acid (PAA) and polyacrylamide (PAM) were chosen as polymerized HBDs, and four types of PDESs were synthesized using choline chloride as HBA. These novel PDESs were impregnated as membrane liquids in the SLMs. The performance of the synthesized SLMs was evaluated with the CO₂ permeability and CO₂/CH₄ selectivity to estimate the practical implication of these SLMs. The effect of operating conditions on membrane separation performance was also analyzed.

TABLE 1 | Composition and nomenclature of the synthesized PDESs.

Composition	Molar ratio (HBD:HBA)	Code	Chemical structure
ChCl/PAA	15:1	PDES-1	
ChCl/PAA	20:1	PDES-2	
ChCl/PAM	15:1	PDES-3	
ChCl/PAM	20:1	PDES-4	

MATERIALS AND METHODS

Choline chloride ($\geq 99\%$), polyacrylic acid (M_n 1,500 g mol^{-1}), poly acrylamide (M_n 1,000 g mol^{-1}) were used in the synthesis of PDES. Polyvinylidene difluoride (PVDF) and N-Methyl-2-Pyrrolidone (NMP) were used to prepare membrane support. Sigma Aldrich supplied all materials. Chemicals were used as provided by the company.

Synthesis of PDESs

PDESs were prepared using the choline chloride (ChCl) as HBA and the polymers-HBDs (PAA and PAM) in two different molar ratios of 15:1 and 20:1, respectively. In a typical procedure, HBD and HBA were mixed in a suitable amount in a sample bottle using a magnetic stirrer. The mixture was heated to 80°C with continued stirring. A homogeneous viscous liquid (PDES) was obtained at the end of 30 min of simultaneous heating and stirring. The mixture was kept under the same reaction conditions for 2 h to ensure complete conversion. By repeating the similar procedure, four different PDESs were synthesized. The composition and nomenclature of the PDESs are presented in Table 1.

SLM Fabrication

PDES-SLMs were prepared by using a PVDF ultrafiltration membrane as a support material. The phase inversion method was used to prepare PVDF membrane support. 15 wt% solution of PVDF was mixed with NMP and stirred for 24 h. Subsequently, a clear homogenous solution was formed that was then casted using Elcometer. 250 μm thickness was maintained during the casting process, and a cast film was formed. The phase transformation was accomplished by dipping the cast membrane in a nonsolvent (water) coagulation bath for 10 min to ensure the complete phase inversion. The synthesized membrane support was placed in a desiccator for 24 h to remove any volatile or water content present. The PVDF membrane sheet was placed in the desiccator overnight to ensure the complete drying to facilitate the incorporation of the PDES liquid on to the surface of the porous membrane. Subsequently, the SLM-1 based on PDES-1 was prepared using the impregnation method. In this typical method, 3 ml of the PDES-1 liquid was evenly spread on the surface of the PVDF

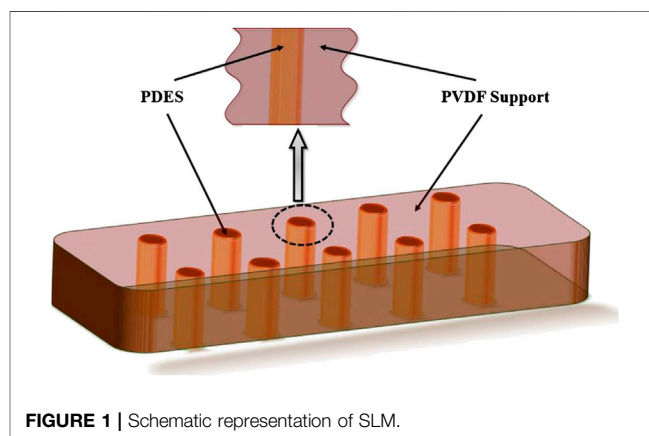
support. Afterward, the membrane was placed in the circular permeation cell at 2 bar nitrogen pressure for 1 h to ensure the impregnation of the PDES-1 into the pores of the PVDF support. As evidence of complete impregnation, a thin layer of the PDES-1 was obtained at the bottom of the PVDF support. The same method was adopted for preparing SLM-2, SLM-3, and SLM-4 based on the corresponding PDES-2-4. The schematic image of synthesized SLMs is presented in Figure 1.

Characterization Techniques

The interaction between HBD and HBA has been confirmed through Fourier Transform Infrared (FTIR) spectroscopy. The FTIR spectra of the HBD and HBA and the PDESs were obtained in a scan range of 4000–800 cm^{-1} at room temperature with a resolution of 8 cm^{-1} . The FTIR spectra were taken using Thermo-Nicolet (6700P) FTIR Spectrometer (USA). Viscosities of the PDESs are very crucial in deciding their practical applications, particularly as membrane liquid in SLMs. The viscosities of the PDESs were determined at room temperature using Ubbelohde viscometer. The vibrating tube densitometer Krüss DS7800 model was used to measure the density of the PDESs at atmospheric pressure.

Membrane Performance Testing

Gas separation performance of the prepared membranes was tested in a custom-built permeation setup by calculating pure

**FIGURE 1** | Schematic representation of SLM.

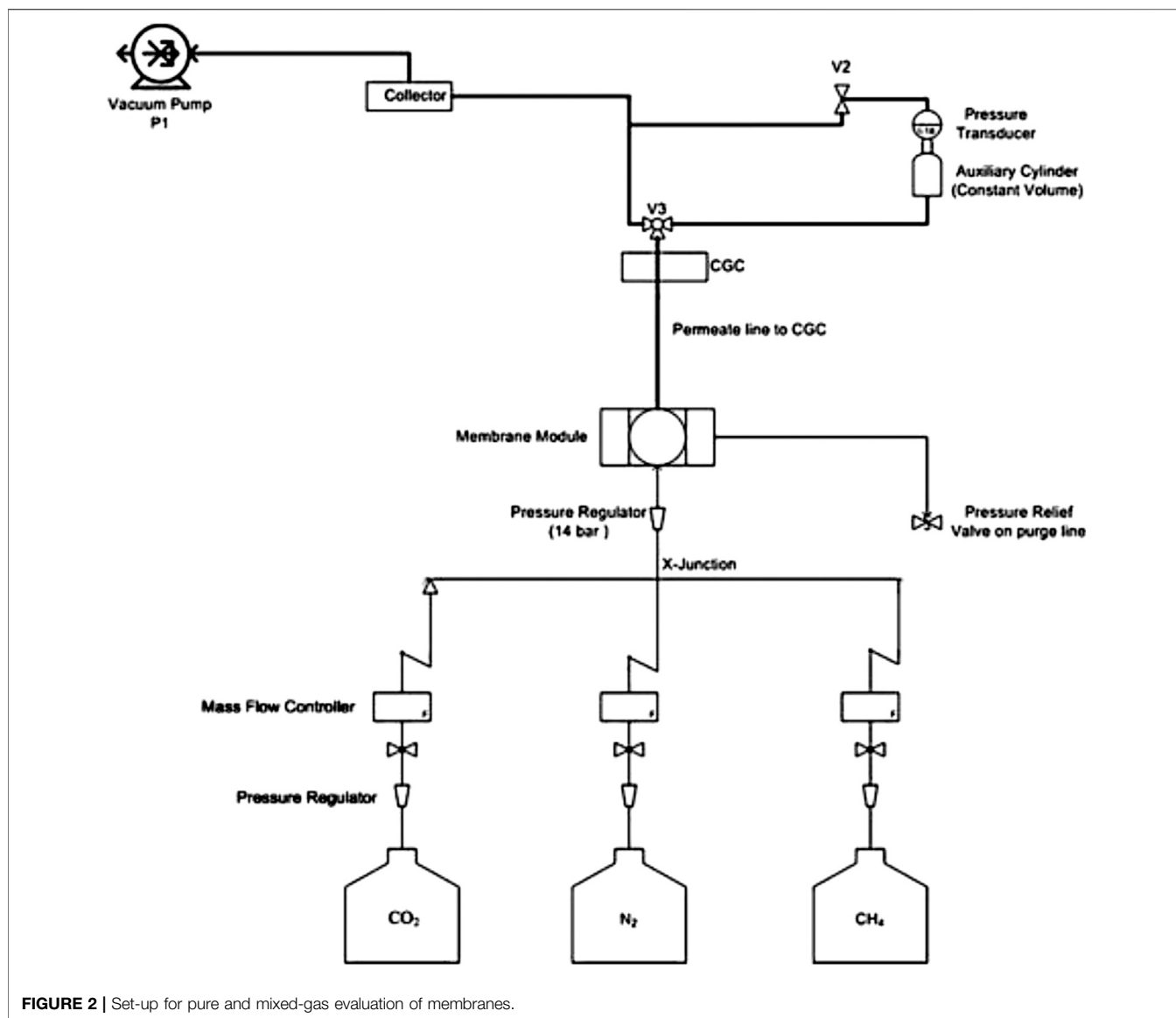


FIGURE 2 | Set-up for pure and mixed-gas evaluation of membranes.

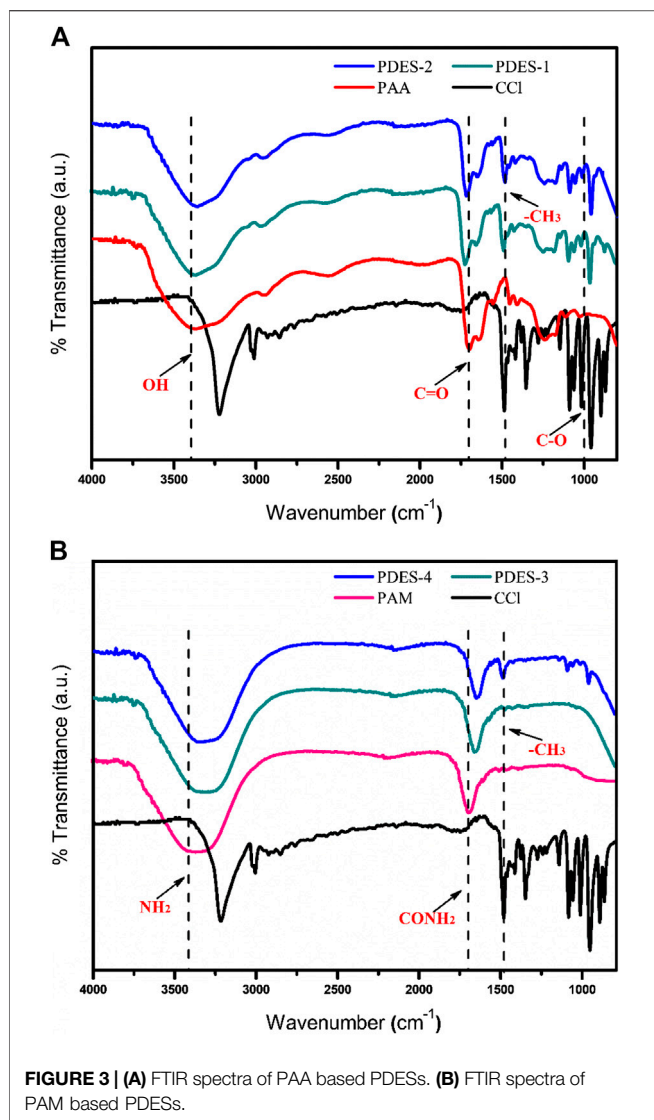
and mixed gas permeabilities and selectivities. Gas permeation was tested at isochoric conditions (constant volume and variable pressure). The pressure of the setup is increased with time. A gas chromatograph equipped with two thermal conductivity detectors, at the front and back of gas chromatograph, was used to analyze the compositions of retentate and permeate. The schematic gas separation setup is shown in **Figure 2**. This setup is constructed of stainless steel. The composition and flow rate of the feed gas is controlled by Mass flow controller. The flow rate could vary from 0 to 1 L/min. The functional area of membrane in single cell permeation setup is 3.8 cm². The working principle and specifications of the setup are defined elsewhere (Khan et al., 2010). The prepared membranes were positioned on the metallic porous support and airtight. The gas feed was introduced at 1 L/min into the

membrane system. The prepared membranes were analyzed within the feed temperature range of 298–338 K to investigate the temperature effect on the gas separation performance. All the experiments were repeated at least three times to eliminate any ambiguity. The SILMs follow the solution diffusion mechanism for the transport of the gasses through them, according to this model

$$J = DS, \quad (1)$$

where J Permeability, D Diffusion Coefficient, S Solubility Coefficient.

The time lag method was adopted to calculate “ D ” and “ S ” (Crank, 1975; Ash and Barrie, 1986). In this method, a high vacuum is applied at one side of the test gas, and D is calculated by calculating the lag time before the steady-state is achieved.



An auxiliary cylinder of 50 cm³ equipped with a pressure transducer that records the rate of increase in pressure is joined to a vacuum pump by valve *V*. The test gas was fed from one side of the cylinder while keeping the other side at vacuum until the steady-state achieved. The time lag intercept θ was calculated from the plotted graph of increasing gas pressure on the vacuum side. The following equation was used to calculate “*D*”

$$D = \frac{l^2}{6\theta} \quad (2)$$

where *l* is membrane thickness. After calculating the *D*, the *S* was calculated using Eq. 1. The selectivity of the gas *A* over gas component *B* was calculated using the following equation.

$$\alpha_{A/B} = \frac{P_A}{P_B} \quad (3)$$

RESULTS AND DISCUSSION

Characterization of the PDESs

The FTIR spectra of the DESs and their individual precursors, presented in Figures 3A,B, have confirmed the interaction between individual precursors resulting in the formation of DES. The characteristic peak analysis of the PDESs presented Figure 3 revealed that it is an approximately an overlap of its constituting components. The characteristic peaks of all the individual components did not disappear in the PDESs spectra showing that the structural integrity of these components has been maintained. The characteristic peaks of ChCl obtained at 3,200 cm⁻¹ correspond to hydroxyl (OH bending) group. While the peak obtained at 1,480 cm⁻¹ corresponds to alkyl group present in the structure of ChCl (Ullah et al., 2015). In case of pure PAA, the broad vibrational band observed between 3,200 and 3,600 cm⁻¹ exhibits the OH stretching in all the PAA containing samples. The other important band that appeared at 1,682 cm⁻¹ represents the carbonyl group present in the PAA (Mota-Morales et al., 2013). In case of pure PAM, the band obtained between 3,450 and 3,300 cm⁻¹ represent the amine group (NH₂ stretching). The bands at 1,702 and 1,640 cm⁻¹ attributed to the carbonyl group (C=O) present. (Kumar et al., 2012). The peaks that appeared between 1,300–1,180 cm⁻¹ are ascribed to the C–N–linkage and CH₂ groups (Dumitrescu et al., 2015).

The carboxylic group present in PAA was found to be in its acid form that is reflected in the peaks obtained at 1,736 and 1,711 cm⁻¹, in PDES-1 and PDES-2, respectively (Mota-Morales et al., 2013). This feature revealed that the interaction between the PAA and ChCl was through hydrogen bonding, a characteristic property of the DESs. The band at 1,480 cm⁻¹ in case of pure ChCl is shifted toward shorter wave number as the percentage of ChCl is increased. Interestingly, the NH₂ bands are shifted toward lower wave number, which confirms the formation of the hydrogen bond between the HBA and HBD moieties (Yue et al., 2012). Additionally, it may be observed in case of all the PDESs spectra that the characteristic peaks undergo redshift as the concentration of the choline content is increased in the PDESs. This can be attributed to the strength of H-bond formed between the polymer and the ChCl, i.e., lower the wave number stronger the H-bond (Jiang et al., 2017).

The molar volume (*V*) of CO₂ sorbent is a critical factor in determining the maximum amount of the gas sorbed per unit volume of the sorbent (Camper et al., 2006). Therefore, the molar volume of the PDESs was measured by the experimental values of density using the following equation.

$$V = \frac{M_{\text{PDES}}}{\rho} \quad (4)$$

In the above equation, *M*_{PDES} and ρ are the molar mass and density of the PDESs, respectively. Where the *M*_{PDES} for the prepared PDESs was determined by using the following equation established for the DESs (Abbott et al., 2011; Peng et al., 2014),

$$M_{\text{PDES}} = \frac{X_{\text{HBA}}M_{\text{HBA}} + X_{\text{HBD}}M_{\text{HBD}}}{X_{\text{HBA}} + X_{\text{HBD}}} \quad (5)$$

TABLE 2 | Physical properties of the PDESs.

PDESs code	M_{PDES} (g mol ⁻¹)	Viscosity (cP)	Density (g cm ⁻³)	Molar volume (cm ³ mol ⁻¹)
PDES-1	224.64	439.01	1.21	185.65
PDES-2	204.4	418.24	1.19	171.76
PDES-3	193.39	387.40	1.14	169.64
PDES-4	180.59	353.66	1.11	162.69

where X and M represent the mole ratio and molar mass (g mol⁻¹) of the HBAs and HBDs, respectively. The physical properties of the prepared PDESs are presented in **Table 2**. The viscosity and density, being the critical parameters for SLM fabrication, were measured three times with great care, and the average of the values are displayed. It can be observed from **Table 2** that the prepared PDESs are moderately viscous. However, these values are lower and comparable to most of the ILs and DESs (García et al., 2015).

Performance of Synthesized PDES-SLMs

The gas performance of the synthesized PDES-SLMs was analyzed by using pure gases CO₂, N₂, and CH₄, and the results are presented in **Table 3**. The solution-diffusion mechanism is responsible for the transport of CO₂ through the SLMs. It is a three-step mechanism in which the CO₂ is first dissolved in the impregnated liquid, diffuses through it, and then for the concentration gradient, is desorbed to the permeate side of the SLMs. The CO₂/CH₄ and CO₂/N₂ selectivities for both types of SLMs were found to be significantly higher between 45.37–50.71 and 56.05–60, respectively. In the case of CO₂/CH₄, the SLM-2 membrane showed the highest selectivity, and for CO₂/N₂, the SLM-4 was the membrane with the highest selectivity. These significantly high selectivities can be attributed to the high solubility of the CO₂ in the DESs (Abbott et al., 2004; García et al., 2015; Aissaoui et al., 2017). The selectivity results can also be justified on the ground of kinetic diameter of the analyzed gases (de Almeida Quintino, 2014). The PDES-SLMs prefer the permeation of small molecules and renders large molecules to pass through the membrane. The kinetic diameter of CO₂ (3.30 Å) is small as compared to the N₂ (3.64 Å) and CH₄ (3.80 Å) that favors the improved selectivity of CO₂/CH₄ and CO₂/N₂. Moreover, the higher values of selectivity may also be ascribed to the lower molar volume of the prepared PDESs. This can be satisfactorily explained by using Camper model (Scovazzo, 2009), according to which the solubility of CO₂ is higher in low molar volume liquids. The molar volume of the prepared PDESs presented in **Table 2** has lower values than most of the commercially used ILs (Scovazzo, 2009). Interestingly, it

can be observed from **Table 3** that the CO₂/CH₄ and CO₂/N₂ selectivities were found to be increased by increasing the ChCl molar ratio. The increase in selectivity can be explained based on molar free volume and the basicity of the DESs (Trivedi et al., 2016; Ghaedi et al., 2017b). It is well established that the molar free volume and basicity of the DESs increase on par with the ChCl content in the DESs (Abbott et al., 2017). The increase in the molar free volume and basicity of the DES give rise to the permeability of the CO₂, which resulted in high values of selectivities.

The acid gas permeability through the prepared SLMs can be illustrated using the hole theory explained by Abbott and coworkers (Abbott et al., 2007). According to this theory, free spaces between the individual ionic moieties of the PDES permit the ions to move through it. Ion-HBD interactions control the size of these holes (Abbott et al., 2007). The PAA based SLMs (SLM-1 and SLM-2) showed notable CO₂ permeability of the order 19.45 and 19.9 Barrer, respectively. The permeability of these novel PDES-SLMs is comparable to the first-ever reported PIL membranes, which were in the range of 9–32 Barrer (Bara et al., 2007). Although the viscous membrane liquids are generally assumed to have lower CO₂ permeability values (Scovazzo, 2009), the prepared PDESs have shown significant CO₂ permeability values. This can be ascribed to the high solubility of the acid gas in the membrane liquid, as the molecular interaction is mainly assumed to govern the permeability rather than the bulk properties (Iarikov et al., 2011). This can also be supported by the reduced permeability values of CH₄ and N₂, as witnessed in the case of permeability results presented in **Table 3**. Moreover, the PAM based SLMs coded as SLM-3 and SLM-4 exhibited higher permeabilities than the SLM-1 and SLM-2. These SLMs showed significantly higher CO₂ permeability values than most of the functionalized imidazolium-based PIL membranes (Bara et al., 2008a; Horne et al., 2015). The SLM-4 showed the maximum CO₂ permeability of the order of 25 Barrer. The reason for this high permeation is the higher solubility, lower molar volumes, and moderate viscosities than the PAA based PDESs (SLM-1,2), as enlisted in **Table 2**.

TABLE 3 | CO₂/CH₄ and CO₂/N₂ ideal gas permeability and selectivity.

SLMs code	Permeability (Barrer)			Selectivity	
	CO ₂	CH ₄	N ₂	P _{CO2} /P _{CH4}	P _{CO2} /P _{N2}
SLM-1	20.56	0.42	0.37	48.95	55.57
SLM-2	21.3	0.42	0.38	50.71	56.05
SLM-3	24.5	0.54	0.43	45.37	56.98
SLM-4	27	0.58	0.45	46.55	60.00

TABLE 4 | CO₂/CH₄ and CO₂/N₂ mixed gas permeability and selectivity.

SLMs code	Permeability (Barrer)			Selectivity	
	CO ₂ (Barrer)	CH ₄ (Barrer)	N ₂ (Barrer)	P _{CO2} /P _{CH4}	P _{CO2} /P _{N2}
SLM-1	19.45	0.40	0.37	47.50	52.57
SLM-2	19.9	0.40	0.38	49.25	52.37
SLM-3	23.4	0.54	0.42	43.22	55.71
SLM-4	25	0.58	0.45	44.03	55.56

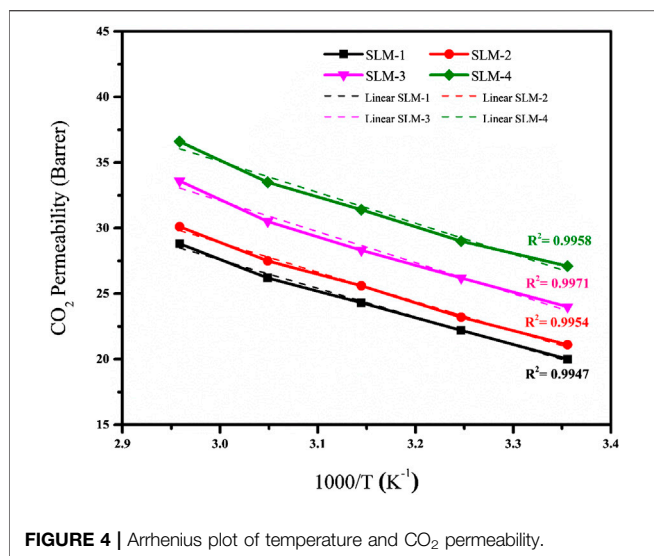


FIGURE 4 | Arrhenius plot of temperature and CO₂ permeability.

The increase in ChCl concentration increases the intermolecular interactions (H-bonding) between the ChCl and HBD polymers, as anticipated in the FTIR spectra presented in **Figures 3A,B**. Therefore, the CO₂ permeability of the PDESs is expected to decrease at higher ChCl concentrations because of stronger intermolecular interactions between the PDES moieties, which in turn reduced the attraction for third moiety CO₂. On the contrary, the CO₂ permeability was found to be increased, instead of decreasing, on a par with ChCl concentration in both types of HBDs, i.e., 20.5 to 21.3 in PAA-SLMs and 24.5 to 27 Barrer for PAM-SLMs when ChCl mole ratio was increased from 15 to 20. This peculiar behavior of CO₂ permeability of the PDES-SLMs could be explained better through Lewis acid-base relation of the acid gas and the PDESs. It is well established that the basicity of the DESs increased to a significant level by increasing the ChCl concentration in the DESs, thereby making the DESs more attractive media for the acid gas capture (Abbott et al., 2017).

The mixed gas (50/50 wt%) permeability and the selectivity results were also evaluated, and the results are presented in **Table 4** to prove the application of the DESs on a commercial scale. The permeability of the CO₂ for polymeric membranes is generally reduced under mixed-gas conditions because of the competitive sorption through the membranes. This competitive phenomenon also lowers the selectivity because of the hindrance created by the CH₄ and N₂ molecules. Interestingly, the mixed gas results for SLMs were not significantly different from the pure gas measurements. This could be attributed to the fact that solubility selectivity governs the membrane selectivity while the gas diffusivity selectivity remains constant for a given gas pair, which is the main difference between supported liquid and polymeric membranes (Condemarin and Scovazzo, 2009). Contrarily, with polymeric membranes, the solubility selectivity remains the same, and diffusivity selectivity governs the overall selectivity of the membrane (Camper et al., 2006). This can be explained by considering the polymer matrix swelling, which alters the diffusivity in polymeric membranes while the diffusivity selectivity performs an insignificant role in case of SLMs.

TABLE 5 | Activation energies of the PDES-SLMs.

Membrane code	Activation energy— E_a (KJ/mol)
SLM-1	4.34
SLM-2	4.3
SLM-3	4.1
SLM-4	4.04

Effect of Temperature on CO₂ Permeability

The CO₂ permeability through all SLMs is significantly affected by changing the operating temperature, as reflected in **Figure 4**. The CO₂ permeability exhibits Arrhenius behavior with a coefficient of determination (R^2) higher than 0.99 for all of the PDES-SLMs. It is well reported that the solubility of the CO₂ in the DESs decrease with the increment in temperature (Li et al., 2008). Moreover, the solubility selectivity is governing the overall performance on the SLMs. Thus, the permeability is expected to decrease with the rise in the operating temperature. However, the CO₂ permeability, instead of decreasing, increased on par with the temperature for all the synthesized PDESs-SLMs. On average, every SLM exhibited a rise in the CO₂ permeability of the order of 12 Barrer by increasing the temperature in the range of 298–338 K. The maximum increment in the CO₂ permeability was witnessed in the case of SLM-2 of the order of 13.2 Barrer. However, this increment in the permeability can be explained by the viscosity and molar free volume parameters. This increase in permeability can be attributed to the lowering of the viscosities of the PDESs at elevated temperatures (D'Agostino et al., 2011). Moreover, the increase in temperature increases the ionic motions in the PDESs, which in turn increases the chain mobility and the hole size of the PDESs, thereby increasing the permeability of the acid gas through the SLMs. It is a valid argument that the molar free volume of the DESs also increased at the elevated temperatures resulting in the more permeability of the penetrant gas through the SLMs (Ghaedi et al., 2017a). The increment of CO₂ permeability with temperature was also found to be in good agreement with the ILs literature

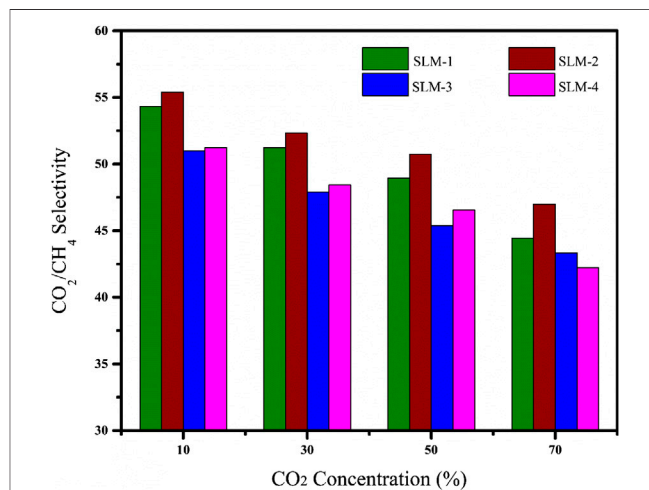
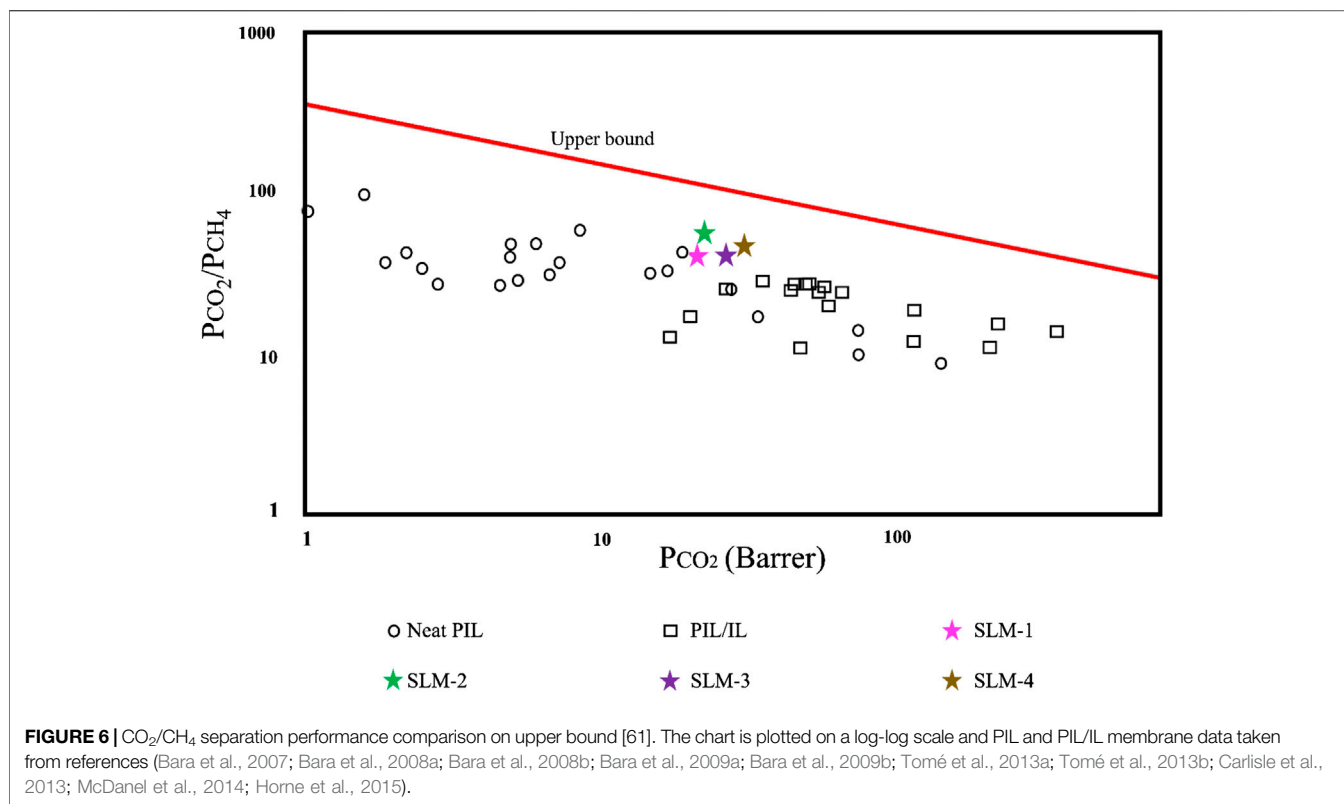


FIGURE 5 | Effect of CO₂ concentration in feed on CO₂/CH₄ selectivity.



(Jindaratsamee et al., 2011; Santos et al., 2014). Therefore, the increase in temperature resulted in an increase in the CO₂ permeability for all PDES-SLMs.

The acid gas permeability was correlated to the feed temperature via activation energy (E_a) in the Arrhenius equation as under

$$P = P_0 \exp(-E_a/RT), \quad (6)$$

where P CO₂ permeability, P_0 pre-exponential factor, R gas constant, T feed temperature.

The activation energies (E_a) of CO₂ permeation for all the PDES-SLMs are listed in Table 5. The PDES-SLMs showed remarkably lower E_a values in the range of 4.04–4.34 kJ/mol. Interestingly, the SLMs E_a values found in this study were significantly lower than most of the reported SILMs using the same PVDF support, which exhibited the E_a values in a range of 16.55–19.37 kJ/mol (Jindaratsamee et al., 2011; Santos et al., 2014). The practical implication of this study and prolific addition to membrane literature is evident from the lower experimental E_a values of the SLMs. It can be observed from Table 5 that the SLM-4 presented the lowest E_a value of 4.04 kJ/mol, thereby making the CO₂ easier to permeate through the membrane. This can be ascribed to the molar free volume and the lower viscosity of the polyacrylamide.

Effect of CO₂ Concentration on CO₂/CH₄ Selectivity

The CO₂ concentration in the feed has a significant effect on the CO₂/CH₄ selectivity, as shown in Figure 5. In CO₂/CH₄ pair, the

selectivity decreased by increasing the CO₂ concentration in the feed from 10 to 70%. The higher values of selectivity at low feed concentration is due to the relative ease of the CO₂ solubility and lesser possibility of matrix swelling by CO₂ plasticization through the PDESs. On increasing the CO₂ concentration from 10 to 70%, the decrease in the selectivity was not significant that supports the argument of the absence of facilitated transport. In facilitated transport, the carriers become saturated at high CO₂ concentration, which enormously lowers the selectivity of the given gas pairs (Bao and Trachtenberg, 2006; Iarikov and Oyama, 2011).

Comparison With PIL Based SLMs With Reported Literature

The gas performance of the synthesized PDES-SLMs and previously reported PIL membrane literature is plotted on the Robeson plot (Robeson, 2008) in Figure 6, which is considered as a benchmark in gauging the performance of the membranes. The Robeson plot is an illustration of ideal selectivity for a given gas pair against permeability of the permeate gas. At the same time, the upper bound line can be viewed as a target for the membrane developers to design new materials (Robeson, 2008). It can be witnessed from Figure 6 that the prepared PDES-SLMs lie very close to the upper bound, characterized by higher selectivities and significantly high CO₂ permeabilities as compared to the neat PIL and PIL/IL composite membranes. Most of the reported neat PIL membranes lie on the top left side, exhibiting significant CO₂/CH₄ selectivities. The very first neat PIL membranes incorporating imidazolium cations on polystyrene and polyacrylate backbone

showed CO₂ permeability as low as nine Barrer and moderate CO₂/CH₄ selectivities from 17 to 39 (Bara et al., 2007). The second generation of the functionalized PIL membranes improved the CO₂ permeability from 8 to 14 Barrers, while reduced CO₂/CH₄ selectivity (29–37) (Horne et al., 2015). The cross-linked PIL membranes showed extremely low CO₂ permeabilities (3.8–4.4 Barrer) for low diffusivity and moderate CO₂/CH₄ selectivities (22–28) (Bara et al., 2008a). The highly permeable PIL membranes were also developed with a permeability of 130 Barrer, although CO₂/CH₄ selectivity was significantly reduced (8.7), which rendered their practical implications where high throughput is required (Carlisle et al., 2013). Conclusively, the functionalization or the variation of cation of neat PIL membranes was not sufficient to endorse the large improvement in gas permeability along with the permselectivity.

These PIL/IL composite membranes were thought to overcome the permeability drawbacks of neat PIL membranes. Incorporating the free IL in PIL matrix increased permeability by approximately 400% as compared to neat PIL membranes (Bara et al., 2008b). However, the CO₂/CH₄ selectivity was reduced to 27, with the difference of minus 25% as compared to the neat PIL membranes (Bara et al., 2008b). The functionalization of free IL with ether, fluoroalkyl, siloxane, alkyl, and nitrile exhibited increased CO₂ permeabilities (47–53 Barrer). However, the CO₂/CH₄ selectivity remained almost unaffected (Bara et al., 2009b). The PIL/IL composite having nitrile group exhibited the highest CO₂/CH₄ selectivity of 28 (Bara et al., 2009b). Besides the functionalization, the amount of free IL was also increased to 50, 60, and 75% to investigate the effect of the concentration of the PIL/IL composite on the gas performance of the membranes (McDanel et al., 2014). The highest CO₂ permeability achieved was 100 Barrer, but the CO₂/CH₄ selectivity was only up to 20. It was concluded that the increase of free IL above a certain level makes the PIL membranes similar to SILMs (McDanel et al., 2014). It is evident from **Figure 6** that the PIL/IL composite membranes also have a severe drawback of reduced selectivity, which makes them impractical in the applications where high purity streams are required.

The PDES-SLMs represents an improvement over the PIL and PIL/IL composite membranes reported in the literature. The synthesized membranes are approaching the upper bound, and systematic research can be targeted to improve the CO₂ permeability while retaining the CO₂/CH₄ selectivity. Besides, the seemingly large combinations of HBAs and HBDs and the tunable nature of the PDESs opens a wide research window in this area. The initial proof of concept for PDES-SLMs is very promising, and novel aspects of this work in synthesizing a green and low-cost substituent of PIL membranes can successfully be achieved with improved acid gas performance as compared to the competitive PIL membrane literature.

Practical Implications of This Study

The membrane technology provides an energy efficient and robust solution for environmental problems. This study focuses on resolving the low permeability and selectivity plus the environmental concerns posed by commonly used CO₂

capturers. The comparison with the previously reported neat PIL and PIL/IL membranes revealed that the novel synthesized PDES-SLM has shown significant improvement in CO₂ permeability and CO₂/CH₄ selectivity. Moreover, another limitation of the membrane based separation systems is the demand of the large surface area. This problem was successfully resolved by the use of yet another membrane module called hollow fiber membrane. The hollow fiber membrane provides a significantly high surface area to volume ratio, and using PDESs in this type of membrane is an interesting idea. This idea has been tested using IL in the hollow fiber module and conceded prolific separation results (Wickramanayake et al., 2013). However, the mechanical stability of the membrane and the drawbacks of IL and rendered the application of these membranes on a commercial scale. The biocompatibility and low cost PDES-SLM should find practical applications in CO₂ sequestering and sweetening of natural gas. The mechanical stability of the suggested membrane system could also be enhanced by applying different membrane fabrication methods and investigating the separation performance under a wide range of pressure (Kim et al., 2011). This study has investigated the novel PDES-SLMs and provided promising results. The practical application of this work would certainly be found by the encouraging idea of using the PDES based hollow fiber membranes.

CONCLUSIONS

A novel study on synthesis, characterization, and the gas separation performance of SLMs using PDESs obtained from already polymerize HBDs is presented. The homogeneous clear solution and FTIR analysis confirmed the formation of the PDESs because of strong hydrogen bonding between the HBAs and HBDs. The PDES prepared herein provided an easy and energy-efficient approach of CO₂ capture by eliminating the complex synthetic steps. The CO₂ permeability of the prepared PDES-SLMs was increased with increasing ChCl content in the PDESs. The SLMs exhibited significantly high values of CO₂ permeability and CO₂/CH₄ selectivity in gas separation experiments. The CO₂ permeability in the PDES-SLMs increased with operating temperature for a decrease in the viscosity of the PDESs at elevated temperatures. The effect of increasing CO₂ concentration in the feed gas mixture proved the absence of facilitated transport in the SLMs. The comparison of the results obtained in this work with the competing literature indicated that PDESs are promising alternatives to the PILs in the membrane-based separations. The present work is one of the very first milestones in this field of PDES based SLM for CO₂ capture. It will open a window of opportunity to design PDESs with task-specific HBD and HBA that might reduce the permeability-selectivity trade-off and surpass the upper-bound.

DATA AVAILABILITY STATEMENT

All datasets presented in this study are included in the article.

AUTHOR CONTRIBUTIONS

All authors listed have made a substantial, direct, and intellectual contribution to the work and approved it for publication.

REFERENCES

- Abbott, A. P., Alabdullah, S. S., Al-Murshedi, A. Y., and Ryder, K. (2017). Brønsted acidity in deep eutectic solvents and ionic liquids. *Faraday Discuss.* 206, 365–377. doi:10.1039/C7FD00153C
- Abbott, A. P., Boothby, D., Capper, G., Davies, D. L., and Rasheed, R. K. (2004). Deep eutectic solvents formed between choline chloride and carboxylic acids: versatile alternatives to ionic liquids. *J. Am. Chem. Soc.* 126 (29), 9142–9147. doi:10.1021/ja048266j
- Abbott, A. P., Capper, G., Davies, D. L., Rasheed, R. K., and Tambyrajah, V. (2003). Novel solvent properties of choline chloride/urea mixtures. *Chem. Commun.* 1, 70–71. doi:10.1039/B210714G
- Abbott, A. P., Harris, R. C., and Ryder, K. (2007). Application of hole theory to define ionic liquids by their transport properties. *J. Phys. Chem.* 111 (18), 4910–4913. doi:10.1021/jp0671998
- Abbott, A. P., Harris, R. C., Ryder, K. S., D'Agostino, C., Gladden, L. F., and Mantle, M. D. (2011). Glycerol eutectics as sustainable solvent systems. *Green Chem.* 13 (1), 82–90. doi:10.1039/C0GC00395F
- Aissaoui, T., AlNashef, I. M., Qureshi, U. A., and Benguerba, Y. (2017). Potential applications of deep eutectic solvents in natural gas sweetening for CO₂ capture. *Rev. Chem. Eng.* 33 (6), 523–550. doi:10.1515/revce-2016-0013
- Ash, R., and Barrie, J. (1986). Time lag in diffusion. *J. Phys. Chem.* 31 (5), 1209–1218. doi:10.1021/j150547a018
- Bao, L., and Trachtenberg, M. (2006). Facilitated transport of CO₂ across a liquid membrane: comparing enzyme, Amine, and Alkaline. *J. Membr. Sci.* 280 (1–2), 330–334. doi:10.1016/j.memsci.2006.01.036
- Bara, J. E., Carlisle, T. K., Gabriel, C. J., Camper, D., Finotello, A., Gin, D. L., et al. (2009a). Guide to CO₂ separations in imidazolium-based room-temperature ionic liquids. *Ind. Eng. Chem. Res.* 48 (6), 2739–2751. doi:10.1021/ie8016237
- Bara, J. E., Hatakeyama, E. S., Gabriel, C. J., Zeng, X., Lessmann, S., Gin, D. L., et al. (2008a). Synthesis and light gas separations in cross-linked gemini room temperature ionic liquid polymer membranes. *J. Membr. Sci.* 316 (1–2), 186–191. doi:10.1016/j.memsci.2007.08.052
- Bara, J. E., Hatakeyama, E. S., Gin, D. L., and Noble, R. (2008b). Improving CO₂ permeability in polymerized room-temperature ionic liquid gas separation membranes through the formation of a solid composite with a room-temperature ionic liquid. *Polym. Adv. Technol.* 19 (10), 1415–1420. doi:10.1002/pat.1209
- Bara, J. E., Lessmann, S., Gabriel, C. J., Hatakeyama, E. S., Noble, R. D., Gin, D. L., et al. (2007). Synthesis and performance of polymerizable room-temperature ionic liquids as gas separation membranes. *Ind. Eng. Chem. Res.* 46 (16), 5397–5404. doi:10.1021/ie0704492
- Bara, J. E., Noble, R. D., and Gin, D. L. (2009b). Effect of “Free” cation substituent on gas separation performance of polymer–room-temperature ionic liquid composite membranes. *Ind. Eng. Chem. Res.* 48 (9), 4607–4610. doi:10.1021/ie801897r
- Bernardo, P., Drioli, E., and Golemme, G. J. (2009). Membrane gas separation: a review/state of the art. *Ind. Eng. Chem. Res.* 48 (10), 4638–4663. doi:10.1021/ie8019032
- Biczak, R., Pawłowska, B., Bałczewski, P., and Rychter, P. (2014). The role of the anion in the toxicity of imidazolium ionic liquids. *J. Hazard. Mater.* 274, 181–190. doi:10.1016/j.jhazmat.2014.03.021
- Camper, D., Bara, J., Koval, C., and Noble, R. J. (2006). Bulk-fluid solubility and membrane feasibility of Rmim-based room-temperature ionic liquids. *Ind. Eng. Chem. Res.* 45 (18), 6279–6283. doi:10.1021/ie060177n
- Carlisle, T. K., Wiesenauer, E. F., Nicodemus, G. D., Gin, D. L., and Noble, R. D. (2013). Ideal CO₂/light gas separation performance of poly (vinylimidazolium) membranes and poly (vinylimidazolium)-ionic liquid composite films. *Ind. Eng. Chem. Res.* 52 (3), 1023–1032. doi:10.1021/ie202305m
- Condemarin, R., and Scovazzo, P. J. C. E. J. (2009). Gas permeabilities, solubilities, diffusivities, and diffusivity correlations for ammonium-based room

ACKNOWLEDGMENTS

AK would like to thank Pakistan Science Foundation (PSF), Pakistan for their Grant No. PSF/Res/P-CIIT/Engg (124).

- temperature ionic liquids with comparison to imidazolium and phosphonium RTIL data. *Chem. Eng. J.* 147 (1), 51–57. doi:10.1016/j.cej.2008.11.015
- Coninck, H., Loos, M., Metz, B., Davidson, O., and Meyer, L. (2005). IPCC special report on carbon dioxide capture and storage. New York: Cambridge University Press
- Crank, J. (1975). *Mathematics of diffusion*. 2nd ed., Chap. iv. Oxford: Clarendon Press.
- D'Agostino, C., Harris, R. C., Abbott, A. P., Gladden, L. F., and Mantle, M. (2011). Molecular motion and ion diffusion in choline chloride based deep eutectic solvents studied by 1 H pulsed field gradient NMR spectroscopy. *Phys. Chem. Chem. Phys.* 13 (48), 21383–21391. doi:10.1039/C1CP22554E
- de Almeida Quintino, E. F. (2014). *A study about CO₂/CH₄ separation using polymeric membranes*. Rio de Janeiro: Universidade Federal do Rio de Janeiro.
- Dumitrescu, A., Lisa, G., Iordan, A., Tudorache, F., Petrilă, I., Borhan, A., et al. (2015). Ni ferrite highly organized as humidity sensors. *Mater. Chem. Phys.* 156, 170–179. doi:10.1016/j.matchemphys.2015.02.044
- Emel'yanenko, V. N., Boeck, G., Verevkin, S. P., and Ludwig, R. (2015). Volatile times for the very first ionic liquid: understanding the vapor pressures and enthalpies of vaporization of ethylammonium nitrate. *Chem. Eur. J.* 20 (37), 11640–11645. doi:10.1002/chem.201403508
- Francisco, M., van den Bruinhorst, A., and Kroon, M. (2013). Low-transition-temperature mixtures (LTTMs): a new generation of designer solvents. *Angewandte Chemie Int. Ed.* 52 (11), 3074–3085. doi:10.1002/anie.201207548
- García, G., Aparicio, S., Ullah, R., and Atilhan, M. (2015). Deep eutectic solvents: physicochemical properties and gas separation applications. *Energy Fuels.* 29 (4), 2616–2644. doi:10.1021/ef5028873
- Ghaedi, H., Ayoub, M., Sufian, S., Lal, B., and Shariff, A. (2017a). Measurement and correlation of physicochemical properties of phosphonium-based deep eutectic solvents at several temperatures (293.15–343.15 K) for CO₂ capture. *J. Chem. Thermodyn.* 113, 41–51. doi:10.1016/j.jct.2017.05.020
- Ghaedi, H., Ayoub, M., Sufian, S., Shariff, A. M., Hailegiorgis, S. M., and Khan, S. N. (2017b). CO₂ capture with the help of Phosphonium-based deep eutectic solvents. *J. Mol. Liq.* 243, 564–571. doi:10.1016/j.molliq.2017.08.046
- Horne, W. J., Andrews, M. A., Shannon, M. S., Terrill, K. L., Moon, J. D., Hayward, S. S., et al. (2015). Effect of branched and cycloalkyl functionalities on CO₂ separation performance of poly (IL) membranes. *Sep. Purif. Technol.* 155, 89–95. doi:10.1016/j.seppur.2015.02.009
- Iarikov, D. D., and Oyama, S. T. (2011). “Review of CO₂/CH₄ separation membranes,” in *Membrane science and technology*. (New York, NY: Elsevier), 91–115.
- Iarikov, D., Hacarlioglu, P., and Oyama, S. (2011). Supported room temperature ionic liquid membranes for CO₂/CH₄ separation. *Chem. Eng. J.* 166 (1), 401–406. doi:10.1016/j.cej.2010.10.060
- Isik, M., Ruiperez, F., Sardon, H., Gonzalez, A., Zulfikar, S., and Mecerreyes, D. (2016a). Innovative poly (ionic liquid) s by the polymerization of deep eutectic monomers. *Macromol. Rapid Commun.* 37 (14), 1135–1142. doi:10.1002/marc.201600026
- Isik, M., Zulfikar, S., Edhaim, F., Ruiperez, F., Rothenberger, A., Mecerreyes, D., et al. (2016b). Sustainable poly (ionic liquids) for CO₂ capture based on deep eutectic monomers. *ACS Sust. Chem. Eng.* 4 (12), 7200–7208. doi:10.1021/acsschemeng.6b02137
- Jiang, B., Dou, H., Zhang, L., Wang, B., Sun, Y., Yang, H., et al. (2017). Novel supported liquid membranes based on deep eutectic solvents for olefin-paraffin separation via facilitated transport. *J. Membr. Sci.* 536, 123–132. doi:10.1016/j.memsci.2017.05.004
- Jindaratamee, P., Shimoyama, Y., Morizaki, H., and Ito, A. (2011). Effects of temperature and anion species on CO₂ permeability and CO₂/N₂ separation coefficient through ionic liquid membranes. *J. Chem. Thermodyn.* 43 (3), 311–314. doi:10.1016/j.jct.2010.09.015
- Khan, A. L., Basu, S., Cano-Odena, A., and Vankelecom, I. (2010). Novel high throughput equipment for membrane-based gas separations. *J. Membr. Sci.* 354 (1–2), 32–39. doi:10.1016/j.memsci.2010.02.069

- Kim, D.-H., Baek, I.-H., Hong, S.-U., and Lee, H.-K. (2011). Study on immobilized liquid membrane using ionic liquid and PVDF hollow fiber as a support for CO₂/N₂ separation. *J. Membr. Sci.* 372 (1–2), 346–354. doi:10.1016/j.memsci.2011.02.025
- Kumar, P., Choonara, Y. E., Toit, L. C. d., Modi, G., Naidoo, D., and Pillay, V. (2012). Novel high-viscosity polyacrylamidated chitosan for neural tissue engineering: fabrication of anisotropic neurodurable scaffold via molecular disposition of persulfate-mediated polymer slicing and complexation. *Int. J. Mol. Sci.* 13 (11), 13966–13984. doi:10.3390/ijms131113966
- Li, X., Hou, M., Han, B., Wang, X., and Zou, L. (2008). Solubility of CO₂ in a choline chloride+ urea eutectic mixture. *J. Chem. Eng. Data.* 53 (2), 548–550. doi:10.1021/je700638u
- Ma, C., Xie, Y., Ji, X., Liu, C., and Lu, X. (2018). Modeling, simulation and evaluation of biogas upgrading using aqueous choline chloride/urea. *Appl. Energy.* 229, 1269–1283. doi:10.1016/j.apenergy.2017.03.059
- Malik, M. A., Hashim, M. A., and Nabi, F. (2011). Ionic liquids in supported liquid membrane technology. *Chem. Eng. J.* 171 (1), 242–254. doi:10.1016/j.cej.2011.03.041
- McDanel, W. M., Cowan, M. G., Carlisle, T. K., Swanson, A. K., Noble, R. D., and Gin, D. (2014). Cross-linked ionic resins and gels from epoxide-functionalized imidazolium ionic liquid monomers. *Polymer* 55 (16), 3305–3313. doi:10.1016/j.polymer.2014.04.039
- Meine, N., Benedetto, F., and Rinaldi, R. (2010). Thermal stability of ionic liquids assessed by potentiometric titration. *Green Chem.* 12 (10), 1711–1714. doi:10.1039/C0GC00091D
- Mota-Morales, J. D., Gutiérrez, M. C., Ferrer, M. L., Sanchez, I. C., Elizalde-Peña, E. A., Pojman, J. A., et al. (2013). Deep eutectic solvents as both active fillers and monomers for frontal polymerization. *J. Polym. Sci. Part A: Polym. Chem.* 51 (8), 1767–1773. doi:10.1002/pola.26555
- Pan, H., Liu, Y., Xia, Q., Zhang, H., Guo, L., Li, H., et al. (2020). Synergetic combination of a mesoporous polymeric acid and a base enables highly efficient heterogeneous catalytic one-pot conversion of crude Jatropha oil into biodiesel. *Green Chem.* 22 (5), 1698–1709. doi:10.1039/C9GC04135D
- Peng, Y., Li, Y., Ban, Y., Jin, H., Jiao, W., Liu, X., et al. (2014). Metal-organic framework nanosheets as building blocks for molecular sieving membranes. *Science* 346 (6215), 1356–1359. doi:10.1126/science.1254227
- Pham, T. P. T., Cho, C.-W., and Yun, Y.-S. (2010). Environmental fate and toxicity of ionic liquids: a review. *Water Res.* 44 (2), 352–372. doi:10.1016/j.watres.2009.09.030
- Ren'ai, L., Zhang, K., Chen, G., Su, B., Tian, J., He, M., et al. (2018). Green polymerizable deep eutectic solvent (PDES) type conductive paper for origami 3D circuits. *Chem. Commun.* 54 (18), 2304–2307. doi:10.1039/C7CC09209A
- Robeson, L. M. (2008). The upper bound revisited. *J. Membr. Sci.* 320 (1–2), 390–400. doi:10.1016/j.memsci.2008.04.030
- Santos, E., Albo, J., and Irabien, A. (2014). Acetate based supported ionic liquid membranes (SILMs) for CO₂ separation: influence of the temperature. *J. Membr. Sci.* 452, 277–283. doi:10.1002/cssc.201600987
- Sarmad, S., Mikkola, J. P., and Ji, X. (2017). Carbon dioxide capture with ionic liquids and deep eutectic solvents: a new generation of sorbents. *Chem. Sust. Chem.* 10 (2), 324–352. doi:10.1002/cssc.201600987
- Scovazzo, P. (2009). Determination of the upper limits, benchmarks, and critical properties for gas separations using stabilized room temperature ionic liquid membranes (SILMs) for the purpose of guiding future research. *J. Membr. Sci.* 343 (1–2), 199–211. doi:10.1016/j.memsci.2009.07.028
- Shen, Y., and Hung, F. (2017). A molecular simulation study of carbon dioxide uptake by a deep eutectic solvent confined in slit nanopores. *J. Phys. Chem. C* 121 (44), 24562–24575. doi:10.1021/acs.jpcc.7b07315
- Shen, Z., Cai, Q., Yin, C., Xia, Q., Cheng, J., Li, X., et al. (2020). Facile synthesis of silica nanosheets with hierarchical pore structure and their amine-functionalized composite for enhanced CO₂ capture. *Chem. Eng. Sci.* 217, 115528. doi:10.1016/j.ces.2020.115528
- Smith, E. L., Abbott, A. P., and Ryder, K. S. (2014). Deep eutectic solvents (DESs) and their applications. *Chem. Rev.* 114 (21), 11060–11082. doi:10.1021/cr300162p
- Songolzadeh, M., Soleimani, M., Takht Ravanchi, M., and Songolzadeh, R. J. (2014). Carbon dioxide separation from flue gases: a technological review emphasizing reduction in greenhouse gas emissions. *Sci. World J.* 2014, 1–14. doi:10.1155/2014/828131
- Tomé, L. C., Abouzadeh, M. A., Rebelo, L. P. N., Freire, C. S., Mecerreyes, D., and Marrucho, I. (2013a). Polymeric ionic liquids with mixtures of counter-anions: a new straightforward strategy for designing pyrrolidinium-based CO₂ separation membranes. *J. Mater. Chem.* 1 (35), 10403–10411. doi:10.1039/C3TA12174G
- Tomé, L. C., Mecerreyes, D., Freire, C. S., Rebelo, L. P. N., and Marrucho, I. (2013b). Pyrrolidinium-based polymeric ionic liquid materials: new perspectives for CO₂ separation membranes. *J. Membr. Sci.* 428, 260–266. doi:10.1016/j.memsci.2012.10.044
- Trivedi, T. J., Lee, J. H., Lee, H. J., Jeong, Y. K., and Choi, J. W. (2016). Deep eutectic solvents as attractive media for CO₂ capture. *Green Chem.* 18 (9), 2834–2842. doi:10.1039/C5GC02319J
- Tuinier, M., van Sint Annaland, M., Kramer, G. J., and Kuipers, J. (2010). Cryogenic CO₂ capture using dynamically operated packed beds. *Chemical Engineering Science.* 65 (1), 114–119. doi:10.1016/j.ces.2009.01.055
- Uchytel, P., Schauer, J., Petrychovyč, R., Setnickova, K., and Suen, S. (2011). Ionic liquid membranes for carbon dioxide–methane separation. *J. Membr. Sci.* 383 (1–2), 262–271. doi:10.1016/j.memsci.2011.08.061
- Ullah, R., Atilhan, M., Anaya, B., Khraisheh, M., García, G., ElKhattat, A., et al. (2015). A detailed study of cholinium chloride and levulinic acid deep eutectic solvent system for CO₂ capture via experimental and molecular simulation approaches. *Phys. Chem. Chem. Phys.* 17 (32), 20941–20960. doi:10.1039/C5CP03364K
- Wang, M., Lawal, A., Stephenson, P., Sidders, J., and Ramshaw, C. J. (2011). Post-combustion CO₂ capture with chemical absorption: a state-of-the-art review. *Chem. Eng. Res. Des.* 89 (9), 1609–1624. doi:10.1016/j.cherd.2010.11.005
- Wickramanayake, S., Hopkinson, D., Myers, C., Sui, L., and Luebke, D. (2013). Investigation of transport and mechanical properties of hollow fiber membranes containing ionic liquids for pre-combustion carbon dioxide capture. *J. Membr. Sci.* 439, 58–67. doi:10.1016/j.memsci.2013.03.039
- Yue, D., Jia, Y., Yao, Y., Sun, J., and Jing, Y. (2012). Structure and electrochemical behavior of ionic liquid analogue based on choline chloride and urea. *Electrochim. Acta.* 65, 30–36. doi:10.1016/j.electacta.2012.01.003
- Zhang, Q., Vigier, K. D. O., Royer, S., and Jerome, F. (2012). Deep eutectic solvents: syntheses, properties and applications. *Chem. Soc. Rev.* 41 (21), 7108–7146. doi:10.1039/C2CS35178A
- Zhang, Y., Ji, X., and Lu, X. (2018). Choline-based deep eutectic solvents for CO₂ separation: review and thermodynamic analysis. *Renew. Sust. Energy Rev.* 97, 436–455. doi:10.1016/j.rser.2018.08.007

Conflict of Interest: The authors declare that the research was conducted in the absence of any commercial or financial relationships that could be construed as a potential conflict of interest.

Copyright © 2020 Ishaq, Gilani, Afzal, Bilad, Nizami, Rehan, Tahir and Khan. This is an open-access article distributed under the terms of the Creative Commons Attribution License (CC BY). The use, distribution or reproduction in other forums is permitted, provided the original author(s) and the copyright owner(s) are credited and that the original publication in this journal is cited, in accordance with accepted academic practice. No use, distribution or reproduction is permitted which does not comply with these terms.